ACS OMEGA

Open Access

http://pubs.acs.org/journal/acsodf

Article

Unveiling the Intermolecular Interactions between Drug 5-Fluorouracil and Watson−Crick/Hoogsteen Base Pairs: A Computational Analysis†

Natarajan Sathiyamoorthy Venkataramanan,* Ambigapathy Suvitha, and Ryoji Sahara*

Cite This: ACS Omega 2024, 9, 24831−24844

Read Online

ACCESS | Metrics & More | Article Recommendations | Supporting Information

ABSTRACT: The adsorption of 5-fluorouracil (5FU) on Watson−Crick (WC) base pairs and Hoogsteen (HT) base pairs has been studied using the dispersion-corrected density functional theory (DFT). The adsorption, binding energy, and thermochemistry for the drug 5FU on the WC and HT base pairs were determined. The most stable geometries were near planar geometry, and 5FU has a higher preference for WC than HT base pairs. The adsorption energies of 5FU on nucleobase pairs are consistently higher than pristine nucleobase pairs, indicating that nucleobase pair cleavage is less likely during the adsorption of the 5FU drug. The enthalpy change for the formation of 5FU−DNA base pairs is higher than that for the formation of 5FU−nucleobases and is enthalpy-driven. The E_{gap} of AT base pairs is higher, suggesting that their chemical reactivity toward further reaction would be less than that of GC base pairs. The electron density difference (EDD) analysis shows a significant decrease in electron density in aromatic regions on the purine bases (adenine/guanine) compared to the pyrimidine bases. The MESP diagram of the stable 5FU−nucleobase pair complexes shows a directional interaction, with the positive regions in a molecule interacting with the negative region of other molecules. The atoms in molecule analysis show that the $\rho(r)$ values of C═O···H−N are higher than those of N···H/N−H···O. The N···H intermolecular bonds between the base pair/drug and nucleobases are weak, closed shell interactions and are electrostatic in nature. The noncovalent interaction analysis shows that several new spikes are engendered along with an increase in their strength, which indicates that the H-bonding interactions are stronger and play a dominant role in stabilizing the complexes. Energy decomposition analysis shows that the drug−nucleobase pair complex has a marginal increase in the electrostatic contributions compared to nucleobase pair complexes.

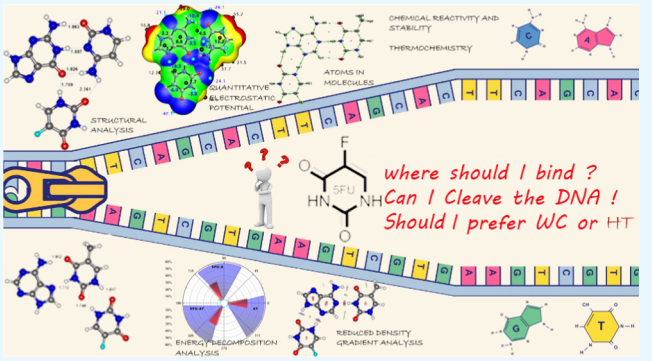

1. INTRODUCTION

Cancer is a complex disease that affects millions of people and is the second-leading cause of death worldwide.[1,2] It involves abnormal biological cell growth with the potential to spread to various parts of the body. Generally, compounds comprising a ribose or 2-deoxyribose sugar ring and purine (adenine (A) and guanine (G)) or pyrimidine (cytosine (C), thymine (T), and uracil (U)) bases were extensively used as anticancer and antiviral therapeutics.[3] Among the pyrimidine analogues, 5-fluorouracil (5FU) and gemcitabine are widely used in the treatment of a variety of solid tumors.[4] 5FU is an antimetabolite drug synthesized by replacing the hydrogen atom in uracil with the fluorine atom at the carbon-5 position of the pyrimidine.[5] The mechanism of action of the cytotoxicity of 5FU involves its incorporation into DNA and RNA through inhibition of thymidylate synthase.[6,7] In the past, several potential sites of the antitumor activity of 5FU have been reported, but the precise mechanism of its action remains unclear. Studies have proven that the toxic effect/resistance of 5FU is due to the misincorporation of 5FU and its metabolite 5-fluoro-2′-deoxyuridine 5′-triphosphate into DNA.[8,9] In the meantime, understanding the mechanism of resistance to 5FU by tumor cells at the molecular level is vital to improving the efficacy of the drug.

It is well established that DNA and RNA are stabilized by hydrogen bonds between the purine and pyrimidine nucleic bases with double-helix and single-stranded geometry, respectively. James Watson and Francis Crick reported the double-helix structure for DNA, with adenine (A) pairing with thymine (T) and guanine (G) pairing with cytosine (C), forming the Watson−Crick (WC) base pairs.[10] Later, Hoogsteen proposed different geometrical orientations, suggesting base pairs between A with T and G with C+,

Received: February 18, 2024
Revised: May 9, 2024
Accepted: May 14, 2024
Published: May 31, 2024

where C+ is the protonated cytosine, referred to as Hoogsteen (HT) base pairs.[11] Advanced dispersion NMR experiments have shown the transient and non-negligible presence of HT base pairs in naked duplex DNA.[12] Furthermore, HT base pairs are hypothesized to play important roles in replication by DNA polymerase, recognition by transition factors, and binding to small molecules.[13]

In general, chemotherapy drugs are categorized as either groove binders or intercalators of DNA, which can result in changes in the parameters of the duplex structure, leading to therapeutic effects.[14] Previous studies have shown that flat molecules interacting from the minor groove side eject the mismatched DNA bases and bind through π-stacking.[15] In the intercalation mode, small molecules are included between the two base pairs of DNA, which are not in direct bonding. Recent experimental works have shown that the intercalation process requires prior formation of noncovalent binding at minor groove sites.[16] The intercalation process is kinetically controlled and slower than minor groove binding, which occurs rapidly.[17] Altogether, the direction of equilibrium is related to the strength of the hydrogen bonds and other weak interactions between groove binders and DNA.[18]

In the past 20 years, computational studies have been aiming at modeling the interactions between DNA nucleobase pairs.[19−23] Using density functional theory (DFT), the tautomerization and protonation of adenine···cytosine mismatches were reported in the gas phase and water.[24] Wang and co-workers investigated the infrared spectroscopy and nuclear-vibrating patterns of multiple H-bonds in WC DNA base pairs using DFT calculations and observed the existence of H-bond cooperativity in them.[25] The interconversion of HT to WC conversion was studied using the restrain-free-energy perturbation-release method, in which HT base pairing was more stable by 2.25 kcal mol^{-1} than the anticonformation.[26] The interaction of hydroxyurea and 5FU with WC base pairs was studied using DFT methods.[27] The drugs were found to bind strongly with the base pairs through hydrogen bonds and alter the geometry of base pairs.[28] The 5FU molecule has the largest interaction energy with the GC base pair and the least with the AA base pair. Wang and co-workers studied the interaction of 4-thiouracil with four RNA nucleobases using the MP2 method.[29] Later studies of 5FU with DNA bases show that 5FU has a higher binding energy with adenine and less with cytosine.[30] The DFT studies on the interaction of 5FU with pyrimidine bases propose that the strongest interaction is between 5FU and cytosine.[31] Later studies on 5FU interaction with DNA base pairs using quantum chemical tools reveal that the 5FU−GC complexes are more stable than the 5FU−AT complex.[32] Recently, halogen-based anticancer agents with intercalating and groove-binding properties with DNA nucleobases were studied using the DFT method.[33] Very recently, Rezaei-Sameti and Iraji Borojeni studied the interaction of 5FU with nucleobases using DFT and TD-DFT methods.[34]

Although there are studies on the adsorption of 5FU drugs on nucleobases and nucleobase pairs, the majority of these studies mainly focus on the energies of absorption. A theoretical study on the nature of interaction between the 5FU drug and nucleobase pairs is still blank. In order to gain a deeper insight and systematic understanding of the nature of the interaction of 5FU with nucleobase pairs, calculations were carried out with an unbiased search on the minimum energy geometry using dispersion-corrected density functional theory (DFT). The nature of the H-bonding interaction was analyzed using quantitative molecular electrostatic potential (MESP), quantum theory of atoms in molecules (QTAIM), noncovalent interaction−reduced density gradient analysis (NCI−RDG), and energy decomposition analysis (EDA) for the nucleobase pairs, 5FU−nucleobases, and 5FU−nucleobase pair complexes. Besides, comparative analysis has been carried out to know the variation of intermolecular H-bonds after the complexation of the 5FU drug with nucleobase pairs. We are hopeful that the findings will be favorable for the experimentalists to design new pyrimidine-based anticancer drugs.

2. COMPUTATIONAL DETAILS

In the present work, we have considered all possible modes of interaction of the drug 5-fluorouracil with the WC and HT base pairs and determined the active site of interaction. All density functional calculations, including optimization, were performed using the Gaussian G16 Rev. C.01 program package.[35] For the generation of initial geometries, we used the artificial bee colony algorithm for cluster global optimization (ABCluster).[36,37] Initial optimization was carried out using the M06-2X/6-311+G(d,p) method with Grimme's D3 dispersion correction.[38,39] The Minnesota functional M06-2X are specially designed to account for the dispersion interaction and provide very good performance for thermochemistry for main group elements.[40] To understand the quality of the chosen theoretical method in predicting the ground-state geometry of the 5FU−DNA base pair complexes, we used LC-wHPBE,[40] PBE0,[41] and wB97XD[42] methods. All of the functionals correctly predict the most stable geometry, such as that of the M06-2X-D3 functional.[43] However, different functionals show a change in the order of low-lying geometries.

The binding energy of the drug on the DNA base pairs is calculated by using eq 1

$$E_{\text{bind}} = E_{(\text{FU-DNA-basepair})} - (E_{(\text{FU})} - E_{(\text{DNA-basepair})}) \quad (1)$$

where $E_{(\text{FU-DNA-basepair})}$ is the total electronic energy of the 5-fluorouracil drug−DNA nucleobases complexes. $E_{(\text{FU})}$ and $E_{(\text{DNA-basepair})}$ are the total electronic energies of 5-fluorouracil and the DNA base pair, respectively.[44]

The optimized structures were further subjected to vibrational frequency analysis at the respective optimized methods to conform to the reported minimum energy geometries in real minima on the potential energy surfaces and to arrive at the thermodynamic parameters. The thermodynamic parameters (ΔH, $T\Delta S$, and ΔG) for the most stable model in the gas and solution phases (water and ethanol) were computed at 298 K and 1 atm pressure using eq 2

$$\Delta\text{TP298} = \text{TP(FU-DNA-basepair)} - (\text{TP(FU)} - \text{TP(DNA-basepair)}) \quad (2)$$

where TP = H is the enthalpy and G is the free energy.

To compute and visualize the three-dimensional (3D) surface of quantitative molecular electrostatic potential (MESP), we employed the wave function analysis−surface analysis suite (WFA−SAS).[45,46]

During the calculations, as suggested by Bader et al., the surface was considered with 0.001 au (electrons/Bohr^3) contour of the electronic density.[47,48] The sign in any region depends upon the effects of the nuclei (positive) or the electrons (negative) predominate. When plotted on a

https://doi.org/10.1021/acsomega.4c01545
ACS Omega 2024, 9, 24831−24844

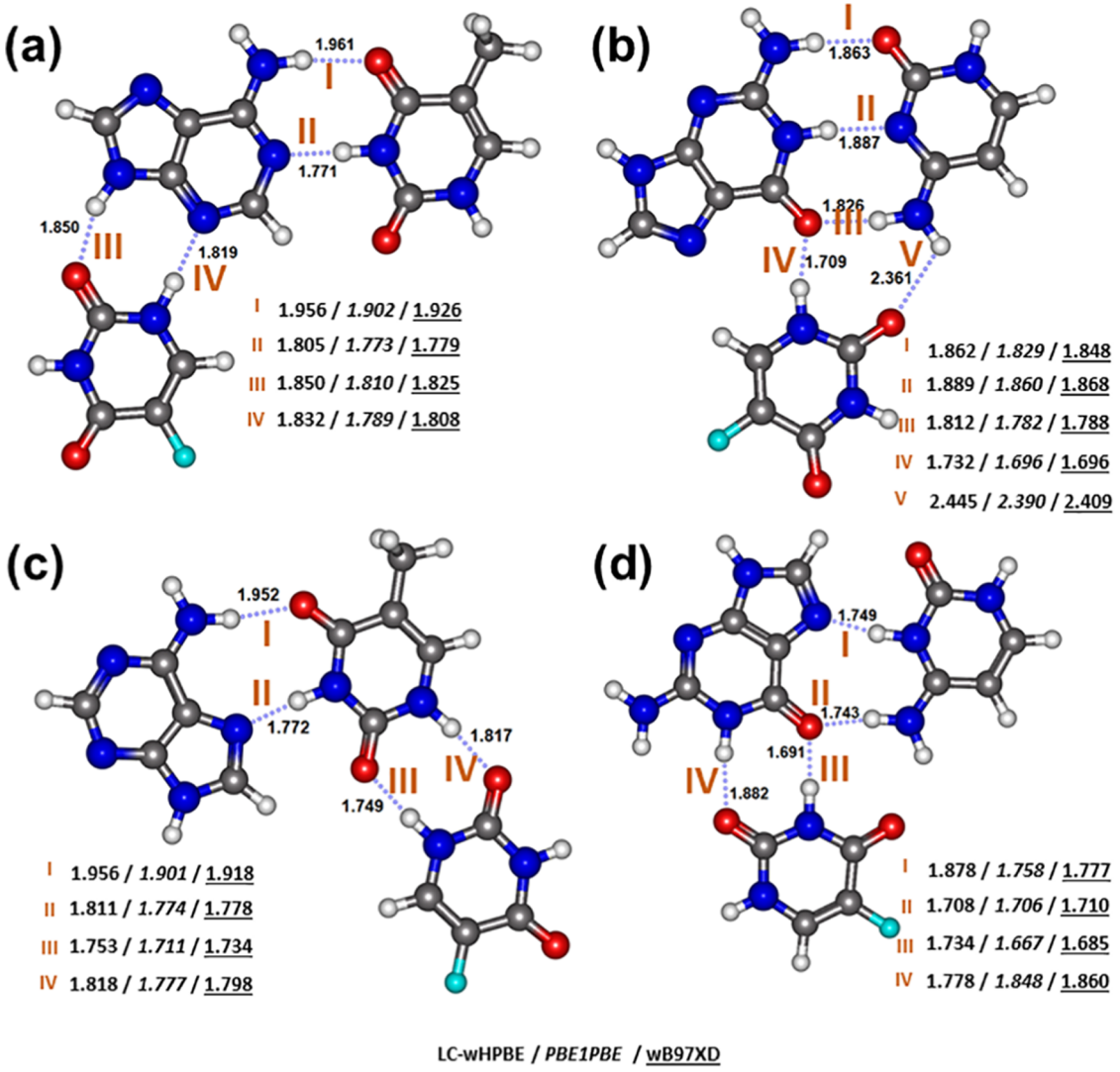

Figure 1. Optimized geometries of the most stable 5FU drug with (a) AT, (b) GC, (c) HAT, and (d) HGC+. The selected H-bond distance (in Angstrom) obtained using the M06-2X functional is provided in the figure. The above H-bond distances obtained using LC-wBPBE (in normal font), PBE0 (in italics), and wB97XD (in underlined fonts) are provided at the bottom of each structure. The number, I, II, III, and IV are the hydrogen bonds between the molecules.

molecular surface, $V(r)$ is designated $V_S(r)$, and its local most positive and most negative values (of which there may be several) are identified as $V_{S,max}$ and $V_{S,min}$, respectively. The ^1H and ^{13}C NMR chemical shifts and the nuclear independent chemical shift (NICS) values of stable complexes were computed in water using the M06-2X/6-311+G(d,p) level of theory using the gauge-independent atomic orbital (GIAO) method.[49,50] The values are obtained by subtracting the reference tetramethylsilane's nuclear magnetic shielding tensors of the proton.[51] Topological parameters were derived with the QTAIM approach using the AIMALL program.[52] Noncovalent interaction (NCI)−reduced density gradient (RDG) analyses were carried out using the Multwfn program and visualized using the ChemCraft program.[53,54] The energy decomposition analysis (EDA) is carried out at the B3LYP-D3/TZVP level of theory using the ADF (2016) program package.[55]

3. RESULTS AND DISCUSSION

3.1. Structure and Geometric Parameters of 5FU−Base Pair Complexes. For a better understanding of the nature of interactions between the drug 5-fluorouracil (5FU) and DNA base pairs (WC and HT), we first examined the most stable interaction geometry with Watson−Crick (WC) and Hoogsteen (HT) base pairs. The drug 5FU was allowed to interact with the DNA base pairs in all possible modes by considering the various active electrophilic and nucleophilic sites of 5FU and WC/HT base pairs.[56] Besides, we also used the artificial bee colony algorithm for cluster global optimization to identify the putative global minimum.[35,36] The WC base pair adenosine−thymine (AT) interacts with 5FU in at least 20 different modes, which are shown in Figure S1 in the Supporting Information. The most stable geometry is shown in Figure 1a, in which 5FU binds to adenosine with N3···H−N and N9−H···O═C bonding. This may be due to the higher acidity on the donor−acceptor sites present in the adenosine and 5FU molecules.[57] In Figure S2, we have provided the various modes of interaction 5FU on adenine

https://doi.org/10.1021/acsomega.4c01545
ACS Omega 2024, 9, 24831−24844

Table 1. Computed Selected Bond Parameters (in Å) for the Stable Complexes and Binding Energy (in kcal mol^{-1}) Using the M06-2X-D3/6-311+G(d,p) Level for the Most Stable 5FU−Nucleobase Pair, 5FU−Nucleobase, and Nucleobase Pair Complexes

	bond distance change (in Å)							
	purine···pyrimidine			5FU···nucleobase				
system	$d_{(N-H\cdots O=C)}$	$d_{(N\cdots H-N)}$	$d_{(N-H\cdots N)}$	$d_{(C=O\cdots H-N)}$	$d_{(C=O\cdots N-H)}$	$d_{(N-H\cdots O=C)}$	$d_{(N-H\cdots N)}$	binding energy (in kcal mol^{-1})
5FU−AT	1.961	1.771	-	-	1.850	-	1.819	−18.90
5FU−GC	1.862	-	1.886	1.826	2.361	1.709	-	−20.97
5FU−HAT	1.952	1.772	-	-	1.817	1.749	-	−17.67
5FU−HGC$^+$	-	1.748	-	1.743	1.882	1.691	-	−23.70
AT	1.942	1.778	-	-	-	-	-	−14.37
GC	1.906	-	1.909	1.774	-	-	-	−27.14
HAT	1.987	1.758	-	-	-	-	-	−14.89
HGC$^+$		1.646	-	1.765	-	-	-	−75.98
5FU−A	-	-	-	-	1.828	-	1.844	−18.03
5FU−G	-	-	-	-	1.922	-	-	−20.39
5FU−T	-	-	-	-	1.762	1.816	-	−18.02
5FU−C$^+$	-	-	-	-	-	-	-	−21.83

along with intermolecular bond parameters. It is interesting to notice that the site of adsorption of 5FU on adenine in the most stable complex is similar to the site of adsorption of the 5FU−AT base pair complex.[32] The intermolecular HBs between 5FU and the AT base pair have bond lengths of 1.819 and 1.850 Å for N3···H−N and N9−H···O=C bonding, respectively, computed at the M06-2X-D3/6-311+G(d,p) level of theory. In the adenine−5FU complex, the above-mentioned bond distances were 1.828 and 1.844 Å, respectively.[34] Thus, the strength of N3···H−N and N9−H···O=C increases and decreases, respectively. The low-lying isomers were found to occur with or without HBs between 5FU and adenine/thymine molecules. Furthermore, in addition to the HBs, many of the low-lying isomers occur with π-stacked interactions, and in the first eight low-lying isomers, the 5FU molecule is bound to the adenine base.

The 5FU interaction with the guanine−cytosine (GC) base pair has at least 18 different modes of interaction, which are shown in Figure S3. The most stable geometry is shown in Figure 1b, in which 5FU interacts with both G and C bases and occurs with cytosine's amine N−H···O and C6=O···H−N HBs, with bond lengths of 2.361 and 1.709 Å, respectively. The first low-lying isomer is found to have $\pi-\pi$ stacking interaction and 1.58 kcal mol^{-1} higher in energy. The second low-lying isomer has 5FU bound to the purine nucleobase and is 1.68 kcal mol^{-1} higher in energy than the most stable geometry. The isomer in which 5FU interacts only with the pyrimidine base is at least 2.61 kcal mol^{-1} higher in energy than the most stable geometry. In Figures S4 and S5, we have provided various modes of interaction of 5FU on guanine and cytosine, respectively. The most stable geometry for the 5FU interaction with guanine has three HBs. Upon the interaction of 5FU with the GC base pair, the intermolecular distance between GC is enlarged by the guanine C=O···H−N cytosine bond, while the other two HBs are reduced. Thus, the 5FU interaction with the GC base pairs leads to anticooperative effects, leading to the stabilization of the complex.[58]

In the interaction of 5FU with the neutral Hoogsteen base pair HAT, we noticed the presence of at least 12 isomers, which are shown in Figure S6. The lowest-energy isomer is shown in Figure 1c. In the above structure, 5FU is bonded to the pyrimidine base, thymine, with N1−H···O=C and C2=O···H−N bonds with bond distances of 1.817 and 1.749 Å, respectively. In Figure S7, we have shown the various modes of interaction of 5FU with thymine bases. In the most stable isomer, the free 5FU−thymine complex has intermolecular bond distances of 1.816 and 1.763 Å. This shows that there is no considerable change in bond length between the 5FU−HAT complex and the free thymine−5FU complex. The first low-lying isomer of the 5FU−HAT complex has a similar geometry as that of most stable isomer but with a change in the carbonyl bonding distance and is 1.25 kcal mol^{-1} higher in energy, while the isomer with 5FU bonded to adenine bases are 0.67 kcal mol^{-1} less stable than the lowest-energy isomer. The 5FU drug molecule interaction with charged Hoogsteen base pair HGC+ leads to eight isomers. The most stable isomer is shown in Figure 1d, while the 7 low-lying isomers are shown in Figure S8. In the most stable isomer, the drug 5FU is bonded to the guanine molecule via N1−H···O=C and C6=O···H−N bonds. In Figure S4, we have shown the various modes of interaction of 5FU with guanine bases. The comparison between the most stable geometry and the structure shown in Figure S4 shows that a bond change has resulted in a low-lying isomer. It is worth pointing out that N1−H, N2−H, and C6=O are the binding sites for the formation of the GC base pair. In the low-lying isomers, the 5FU drug bonds mainly with the guanine base through hydrogen bonding or by π stacking and least prefers to bind with the cytosine base, which exists as a protonated species and holds a positive charge.[59] Previous studies on the binding of 5FU with bases showed that planar structures have higher interaction energy than structures with buckle angles.[34] In the present study, we observe that the interaction of 5FU with base pairs shows that the planar structures were found to have more stability than the structures with buckle angle 5FU, and the intermolecular H-bond distance between base pairs shows the strengthening of some and weakening of other bonds.

To verify the effect of density functionals (DFs) in predicting the lowest-energy geometry, we have optimized all geometries using the long-range corrected Perdew−Burke−Ernzerhof (LC-wPBE) functional, one-parameter hybrid Perdew−Burke−Ernzerhof (PBE0) functional, and a range separated version of Becke's 97 with empirical atom−atom dispersion correction (wB97XD) functional. All of the studied functionals consistently predicted the most stable geometry; however, the order of low-lying isomers differs with different

https://doi.org/10.1021/acsomega.4c01545
ACS Omega 2024, 9, 24831−24844

Table 2. Computed Interaction Energies, Two- and Three-Bond Interaction Energies of a 5-Fluorouracil Molecule on Watson−Crick Base Pairs (AT and GC) and Hoogsteen Base Pairs (HAT and HGC$^+$)[a]

complex	ΔE_{Total}	$\Delta^2E_{(A/G+FU)}$	$\Delta^2E_{(T/C)+FU}$	$\Delta^2E_{(basepairs)}$	Δ^3E
5FU−AT	−35.13	−19.04	1.04	−15.40 (−15.40)	−1.72
5FU−GC	−51.25	−11.71	−2.20	−29.30 (28.76)	−8.03
5FU−HAT	−34.42	2.02	−19.00	−14.99 (15.99)	−2.46
5FU−HGC$^+$	−69.38	−14.90	−8.63	−44.44 (77.07)	−1.41

[a]The values in parentheses are for the nucleobase pairs. All of the parameters are provided in kcal mol^{-1}.

Table 3. Computed Thermodynamic Parameters for the Formation of 5-Fluorouracil−Base Pair Complexes in Various Theoretical Functionals with the 6-311+G(d,p) Basis Set for Stable Complexes[a]

	ΔH				ΔG			
complex	M06-2X-D3	LC-wHPBE	PBE0	wB97XD	M06-2X-D3	LC-wHPBE	PBE0	wB97XD
5FU−AT	−18.45	−16.26	−17.95	−19.35	−7.99	−5.25	−6.80	−8.24
5FU−GC	−20.56	−17.27	−18.52	−21.11	−9.13	−6.50	−7.51	−7.89
5FU−HAT	−17.23	−14.93	−16.69	−17.76	−7.16	−4.18	−5.80	−7.30
5FU−HGC$^+$	−23.25	−19.82	−21.44	−23.82	−12.26	−7.88	−9.96	−12.38

[a]All of the parameters are provided in kcal mol^{-1}.

functionals. The computed intermolecular geometrical parameters using various functionals for the 5FU−base pairs and pristine base pairs are provided in Figures 1 and S9, respectively. In general, the one-parameter hybrid PBE0 functional delivers the shortest distance, and the long-range corrected LC-wHPBE predicts the longest intermolecular distances in the 5FU−base pair and pristine base pair complexes. In the case of 5FU interaction with nucleobases A, G, C, and T, we noticed the presence of several new low-lying geometries, and specifically in the case of the 5FU−A complex, we observed the structure shown in Figure S2(a)in the Supporting Information to have the highest interaction energy. Previous studies by Rezaei-Samatis and Borojeni have found the structure shown in Figure S2(b) to be the lowest-energy isomer. The identification of the new lowest-energy structure for the AT base pair is due to the unbiased search using the artificial bee colony algorithm.[35,37]

As the strength of HBs can be qualitatively estimated from the bond lengths, in Table 1, we have listed the selective intermolecular bond distance in drug 5FU−base pair complexes, pristine bases, and 5FU drug with bases at the complex formation binding site.[60] The stretching vibrational frequencies of the above bonds are presented in Table S1 in the Supporting Information. In the 5FU−AT complex, the intermolecular distance among the purine···pyrimidine bases and the N−H···O═C bond length increase, while the N···H−N distance decreases by a small magnitude. A similar trend has been observed in the intermolecular distance between the drug 5FU and the AT base pair. In the 5FU−GC complex, the intermolecular distance in GC shows a marginal decrease in the bond distance for the N−H···O═C and N···H−N bonds and an increase in bond distance for the C═O···H−N bond. The increase in the C═O···H−N bond can be attributed to the bifurcated bond observed between the bases and drug 5FU.[61] In the Hoogsteen base pair complexes 5FU−HAT and 5FU−HGC$^+$, a trend of an increase in bond length and a simultaneous decrease in bond length of other bonds has been observed, presumably due to the cooperativity effect among the intermolecular bonds. It is evident from Table S1that the stretching frequency of all of the hydrogen bonds shows a decrease, which supports the increase in the strength of H-bonds.

3.2. Energetic Analysis and Choice of Functionals.

The binding energy of the drug 5FU on the nucleobase pair is evaluated using eq 1 and provided in Table 1. In all of the studied complexes, the binding energy values were negative, implying that the formed complexes are stable. The binding of 5FU on base pairs is provided in Table 1, which is in good agreement with other reports.[27,32] Our computed values show that 5FU prefers to bind with guanine and cytosine bases. A comparison between the free nucleobase and DNA nucleobase pairs shows only a marginal increase in the adsorption energy except for the Hoogsteen base pair complex 5FU−HGC$^+$. The computed binding energy on the base pairs using the M06-2X-D3 method for the most stable complexes is in the range from −17.67 to −23.70 kcal mol^{-1}. These observed values are consistent with the previous results of Kolandaivel et al. and Nowroozi et al.[27,32] The higher adsorption of 5FU on HGC$^+$ can be attributed to the cationic nature of the base pair, especially the cytosine exists in the charged state due to the existence of a proton on the 3N nitrogen site of cytosine. A comparison between the adsorption energies of 5FU on WC and neutral HT of AT base pairs shows that the WC model shows a higher preference for the 5FU drug. Besides, the structures with buckle angle 5FU and those with π− interactions were found to have considerably lower stability. A comparison of adsorption energy between the 5FU−nucleobase pairs and 5FU−base pairs shows only a marginal increase in the value. However, the 5FU−nucleobase pairs consistently have higher adsorption energy for the 5FU drug but lower than the pristine nucleobase pairs. This indicates that nucleobase pair cleavage is less likely during the adsorption of the 5FU drug.

The interaction energy ΔE_{total} is computed and listed in Table 2. The interaction energy was highest for the cationic Hoogsteen base pair complex 5FU−HGC$^+$ and least for 5FU−HAT. The WC base pair has interaction energies of −35.13 and −51.25 kcal mol^{-1}, which are consistent with the previous works.[19,20] After applying the basis set superposition error (BSSE) correction, the binding energies of 5FU with the WC base pair were found to be −35.04 and −51.16 kcal mol^{-1}, respectively. It is interesting to notice that the three-body interaction energy (Δ^3E) is small for all of the stable complexes, except for the 5FU−GC base pair complex. The

https://doi.org/10.1021/acsomega.4c01545
ACS Omega 2024, 9, 24831−24844

Table 4. Computed Band Gap (E_{gap}) and the Reactive Descriptors for the Host and Guest Molecules Computed in the Solution Phase at the M06-2X-D3/6-311+G(d,p) Level of Theory[a]

system	HOMO	LUMO	E_{gap}	μ	η	ω	σ	ΔN	ECT
5FU−AT	−7.82	−0.59	7.23	4.21	7.23	1.22	0.14	−0.58	−0.05
5FU−GC	−7.37	−0.65	6.72	4.01	6.72	1.20	0.15	−0.60	0.00
5FU−HAT	−7.62	−0.83	6.78	4.23	6.79	1.31	0.15	−0.62	−0.04
5FU−HGC^+	−10.31	−3.93	6.37	7.12	6.38	3.97	0.16	−1.12	0.58
5FU	−8.69	−0.82	7.87	4.76	7.87	1.44	0.13	−0.60	-
AT	−7.51	−0.33	7.18	3.92	7.18	1.07	0.14	−0.55	-
GC	−6.74	−0.64	6.10	3.69	6.10	1.12	0.16	−0.60	-
HAT	−7.45	−0.43	7.02	3.94	7.02	1.11	0.14	−0.56	-
HGC^+	−10.48	−4.23	6.25	7.36	6.25	4.33	0.16	−1.18	-

[a]All of the values reported are in eV.

two-body interaction terms are higher for the base pair interaction than for the base−drug interaction, except for the Hoogsteen 5FU−HAT complex. Among the base pair interactions, the two-body interaction term ($\Delta^2E_{basepair}$) is highest for the Hoogsteen HGC^+ base pair, presumably due to its cationic nature. A comparison of $\Delta^2E_{basepair}$ before and after 5FU complexation shows a marginal decrease in the interaction energies, except for the cationic 5FU−HGC^+ complex. The drug interaction Δ^2E terms are highest for the AT and HAT complex, while least for the GC complex. This indicates that 5FU can bind to the AT and HAT base pairs more firmly than to the GC and HGC^+ base pairs.

The thermodynamic parameters for the interaction of 5FU with WC and HT base pairs and individual bases are computed using eq 2 and are listed in Tables 3 and S2 (Supporting Information), respectively. From Tables S2 (Supporting Information) and 3, it is evident that the thermodynamic parameters such as enthalpy and Gibbs free energy are all negative for all of the studied complexes. The negative values of enthalpy and Gibbs free energy indicate that 5FU complexation with nucleobase/nucleobase pairs is exothermic and spontaneous. In general, the change in enthalpy for the 5FU−DNA base pair complexes is higher than that for the 5FU−nucleobase complexes. Furthermore, the change in enthalpy is higher for all complexes, indicating that the complex formation is an enthalpy-driven process. Thus, the 5FU drug complexation with DNA base pairs is more facile than on free nucleobases and is an enthalpy-driven process.

The order of change in enthalpy for the complexation of 5FU with base pairs is as follows: 5FU−HCG^+ > 5FU−GC > 5FU−AT > 5FU−HAT. In general, the GC base pairs show a higher change in enthalpy than the AT base pairs. Previously, Razaei-Sameti and Borojeni have observed that cytosine and guanine bases pair have the highest enthalpy with the 5FU drug.[34] By the comparison between the charged and neutral base pairs, the interaction of 5FU shows that the Hoogsteen cationic base pair HGC^+ has the highest enthalpy and free energy change, indicating facile complexation of 5FU with the HGC^+ base pair. Generally, the enthalpy and entropy were found to be in the order of 5FU−nucleobase pairs > 5FU−nucleobase > nucleobase. Thus, the formation of 5FU−nucleobase pairs is more facile than the formation of 5FU−nucleobases. To evaluate the efficiency of different functionals and to benchmark the best method for exploring the energetics of drug interactions with nucleobases, the LC-wHPBE, PBE0, and wB97XD functionals are employed to compute the enthalpy and free energy change. The thermodynamic parameters have the following trend: wB97XD > M06-2X-D3 > PBE0 > LC-wHPBE. Previous studies on the adsorption of 5FU on nucleobases show that the wB97XD/Lanl2DZ method estimates the highest adsorption energy.[34]

3.3. Chemical Reactivity and Stability of Complexes.

During chemical reactions, the highest occupied molecular orbital (HOMO) and the lowest unoccupied molecular orbital (LUMO) are the main orbitals that take part in the reaction. The HOMO embodies the ability to donate an electron, and LUMO decides the ability to accept an electron.[62,63] Thus, the frontier molecular orbital (FMO) gap, namely, the HOMO−LUMO gap in a compound, can be used to predict the electronic stability of the system. Besides, the quantum chemical descriptors that include chemical hardness (η), chemical potential (μ), electrophilicity index (ω), and softness (σ) can be evaluated by using the Koopmans theorem.[64] The above quantum chemical descriptors can be computed using eqs 3−7.

$$\eta = \mathrm{IP} - \mathrm{EA} \approx E_{\mathrm{LUMO}} - E_{\mathrm{HOMO}} \tag{3}$$

$$\mu = -\chi = \frac{(\mathrm{IP} + \mathrm{EA})}{2} \approx \frac{E_{\mathrm{HOMO}} + E_{\mathrm{LUMO}}}{2} \tag{4}$$

$$\omega = \frac{\mu^2}{2\eta} \approx \frac{(E_{\mathrm{HOMO}} + E_{\mathrm{LUMO}})^2}{4(E_{\mathrm{LUMO}} - E_{\mathrm{HOMO}})} \tag{5}$$

$$\sigma = \frac{1}{\mathrm{IP} - \mathrm{EA}} = \frac{1}{\eta} \approx \frac{1}{E_{\mathrm{LUMO}} - E_{\mathrm{HOMO}}} \tag{6}$$

$$\Delta N = -\frac{\mu}{\eta} \tag{7}$$

The computed quantum chemical descriptors for the 5FU−nucleobase pair complexes, 5FU drug, and base pairs are provided in Table 4. The energy gap of the nucleobase pairs was in the range of 6.10−7.18 eV. The 5FU drug has an E_{gap} of 7.87 eV, while the 5FU−nucleobase pair complexes have values in the range of 6.37−7.23 eV. The AT base pairs have higher E_{gap}, which suggests that their chemical reactivity toward further reaction would be less compared to GC base pairs. The chemical hardness is highest for the 5FU−AT complex and follows the trend 5FU−AT > 5FU−HAT > 5FU−GC > 5FU−HGC^+. Thus, the 5FU complexes of AT base pairs are less likely to undergo electron transfer and are less reactive than the GC complexes. A comparison between free nucleobase pairs and the 5FU−nucleobase pairs shows that the latter has a higher value compared to the former, which indicates that 5FU−nucleobase pair complexes are less reactive compared to the free nucleobase pairs. Thus, the

https://doi.org/10.1021/acsomega.4c01545
ACS Omega 2024, 9, 24831−24844

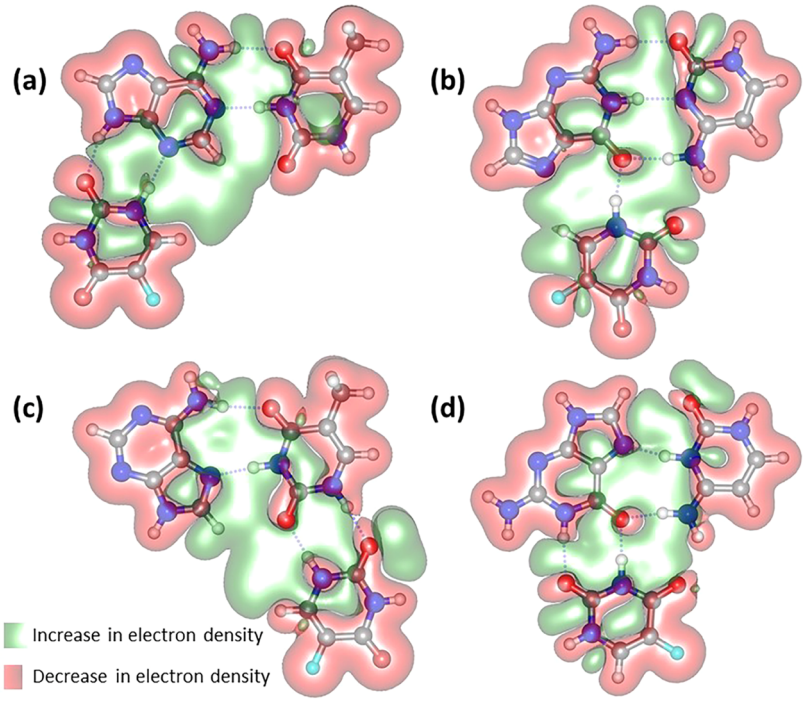

Figure 2. Electron density difference diagram (EDD) for 5FU drug with (a) AT, (b) GC, (c) HAT, and (d) HGC^+ nucleobase pairs.

formed 5FU−nucleobase pair complex's reactivity with another drug molecule is less likely. Besides the hardness, the term softness also supports the prior conclusion on reactivity.

The electrophilicity index (ω) is a positive quantity, and high values are characteristics of most electrophilic systems.[65] Thus, the cationic nucleobase pair and its 5FU complex have the highest electrophilicity index values of 4.33 and 3.97 eV, respectively. From the above value, one can anticipate that the 5FU−HGC^+ complex is less electrophilic than the HGC^+ base pair, which is a consequence of π−electron delocalization between the 5FU drug and the HGC^+ base pair through hydrogen bonds. A comparison between the WC and HT base pair of AT shows that the Hoogsteen base pair has higher electrophilicity. The chemical potential (μ) in a system describes the escaping tendency of an electron cloud.[66] During complex formation, the electrons flow from the higher chemical potential to the lower species until the electronic chemical potential turns out to be equal. The free 5FU drug has a chemical potential of 4.76 eV, while the neutral base pairs have chemical potential values in the range of 3.94−3.64 eV. On the contrary, the cationic nucleobase pair HGC^+ has a chemical potential of 7.36 eV, indicating that it can attract electrons. To understand the direction of charge transfer, we have computed the electrophilicity-based charge transfer using eq 8.

$$\mathrm{ECT} = (\Delta N_{\mathrm{5FU}}) - (\Delta N_{\mathrm{basepair}}) \tag{8}$$

When ECT < 0, 5FU acts as an electron donor, and if ECT > 0, then 5FU acts as an electron acceptor. In the case of 5FU complexes with AT base pairs, ECT values are negative, indicating that electron transfer occurs from the 5FU drug to the base pair, while for the 5FU−GC complex, the ECT was zero, indicating that the net charge transfer is zero. On the contrary, for the cationic 5FU−HGC^+ complex, the ECT value is positive, and hence, 5FU gains electrons from the base pair.

3.4. Nature of Intermolecular Interaction. To realize the charge transfer between the base pair and the 5FU drug and to identify the other intermolecular interactions that are accountable for stabilization, we carried out the electron density difference (EDD),[67] quantitative molecular electrostatic potential (MESP),[68] atoms in molecules (AIM) analysis,[69] noncovalent interaction−reduced density gradient (NCI−RDG) analysis,[70] and energy density decomposition (EDA) analysis.[71] It has been well documented that H-bonding interactions increase the cyclic $4n + 2\pi$ electron delocalization and boost aromaticity. Hence, we have computed the harmonic oscillator model of aromaticity (HOMA) and nucleus-independent chemical shifts (NICS) analysis for the nucleobase pairs and compared it with the 5FU−nucleobase pair complexes to understand how the H-bonding between 5FU and nucleobases affect the bonding between nucleobase pairs.[72]

3.4.1. Electron Density Difference and Molecular Electrostatic Potential Analysis. In the study involving complex formations, the electron density difference (EDD) provides meaningful insights into the characteristics of the nature of the interaction. The EDD is obtained from the difference between the density of the complex to the sum of isolated monomers, namely, the 5FU drug and nucleobase pairs.[73,74] The EDD isodensity surface mapped on an electron density of 0.01 au for the 5FU complexes with WC/HT base pairs is shown in Figure 2. In the figure, the green regions represent the increase in electron density, and the red regions represent the regions with decreased electron density in the complex. The plots suggest that an electron density decrease is observed in the aromatic regions, while an increase in density is observed in the regions where intermolecular hydrogen bonds exist between the drug and DNA base pair/bases. It is obvious from the figure that the oxygen atom of carbonyl groups on pyrimidine bases and 5FU drug lose π electron density, while an increase in σ−electron density is noticed in the amine N−H group. The decrease in

https://doi.org/10.1021/acsomega.4c01545
ACS Omega 2024, 9, 24831−24844

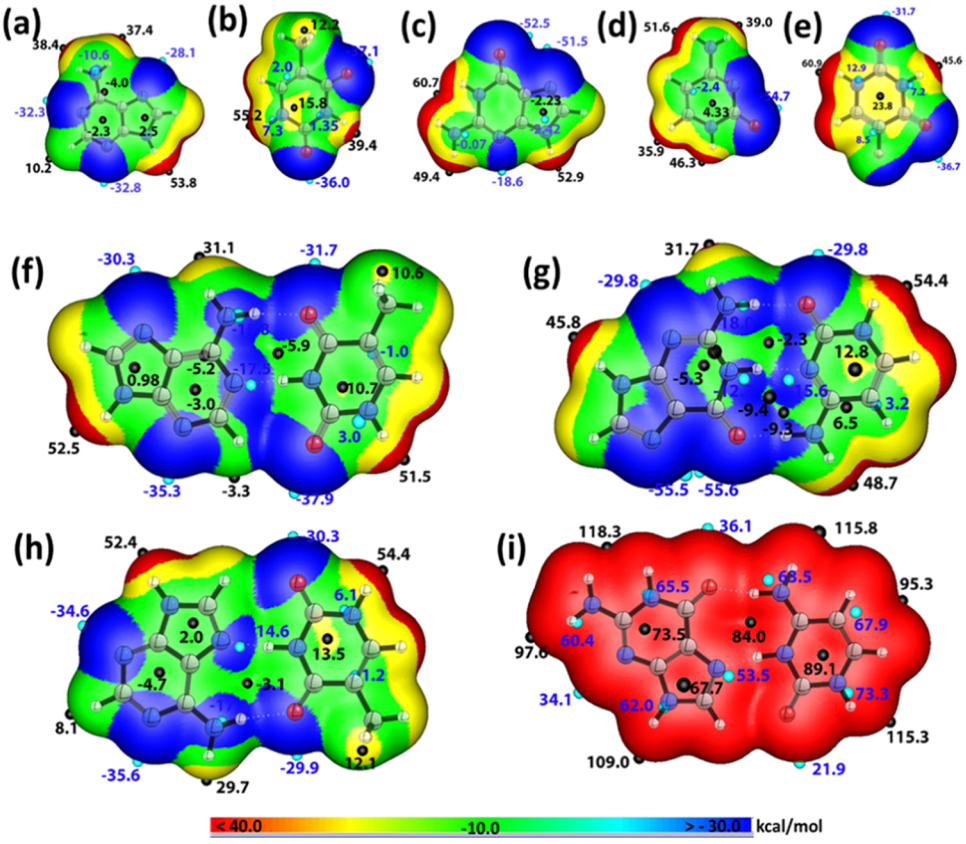

Figure 3. Molecular electrostatic surface potentials mapped on the corresponding 0.001 au electron density isosurface: (a) A, (b) T, (c) G, and (d) C nucleobases, (e) 5FU, and (f) AT, (g) GC, (h) HAT, and (i) HGC^+ nucleobase pairs.

electron density in aromatic regions is more significant on the purine bases (adenine/guanine) compared to the pyrimidine bases, likely due to the extended π-orbital delocalization. This significant delocalization as well as the higher charge transfer highlights the substantial increase in the adsorption of 5FU on the purine bases.

Figure 3 depicts the quantitate electrostatic potentials for the bases, base pairs, and 5FU molecules mapped on a 0.001 electrons/$Bohr^3$ isodensity surface, where red color represents a positive potential designated as $V_{s,max}$ and thus is an electrophilic area, and blue color depicts a more negative potential designated as $V_{s,min}$ and thus is a nucleophilic region.[75,76] The MESP for the 5FU−base pair complexes is provided in Figure S10 in the Supporting Information. In the nucleobases and 5FU molecules, $V_{s,max}$ is observed on the amino group and the hydrogen attached to the pyrrole-like nitrogen atom. The $V_{s,min}$ regions are observed on nitrogen atoms and carbonyl groups. In the DNA base pairs, we notice that the red regions match with the blue regions, forming the base pairs. It is well documented that the proximity of the areas of the same color when brought closer would destabilize the system, and the most stable system will be formed by a directional interaction.[77,78] In the AT base pair, $V_{s,max}$ is observed on the hydrogen atoms of five-membered adenine and six-membered thymine molecules, while $V_{s,min}$ is observed on the nitrogen and oxygen atoms of A and T bases. Analogous to the AT base pair, in the GC and Hoogsteen HAT base pairs, the hydrogen and oxygen atoms own $V_{s,max}$ and $V_{s,min}$, respectively. Interestingly, in the HAT base pair the highest $V_{s,max}$ was observed on the thymine molecule, unlike in the AT base pair in which $V_{s,max}$ is observed on the adenine molecule. In the case of the HGC^+ base pair, as the molecule is positively charged, $V_{s,max}$ and $V_{s,min}$ all were found to hold positive potential. In the drug molecule, the highest $V_{s,min}$ with a value of −36.7 kcal mol^{-1} was observed on the oxygen atom of the carbonyl group adjacent to the fluoride, while the other oxygen atom of carbonyl has $V_{s,min}$ with a value of −31.7 kcal mol^{-1}. The most positive potential was observed on the hydrogen atom of C−H with a value of 60.9 kcal mol^{-1}, while the hydrogen atom of N−H has a value of −45.6 kcal mol^{-1}.

The 5FU drug adsorbed on base pairs is visualized in Figure S10. Due to the directional interaction, the positive regions in a molecule will interact with the negative region, leading to a decrease or increase in the positive or negative values.[79] In the most stable 5FU−AT complex, the $V_{s,min}$ value observed on the oxygen atom of the adenine group is reduced from −35.3 to −6.0 kcal mol^{-1}, the carbonyl oxygen on the 5FU unit attached to the N−H group is reduced from −31.7 to −20.6 kcal mol^{-1}, and the other carbonyl group of the 5FU drug has gained a marginal increase in $V_{s,min}$ value. Similar allusion is observed in all other stable complexes. These indicate that the electron density shift occurs from the 5FU drug, which corroborates with the finding observed in the ECT charge transfer analysis.

3.4.2. π−Electron Delocalization Indicators. Previous studies on the aromaticity of WC base pairs show the increase in the aromatic character of the rings during the H-bond formation involving the carbonyl groups of nucleobases due to cyclic π−electron delocalization.[32] As the complexation of 5FU with a base pair results in a planar structure and the MESP and ECT show a larger charge transfer, we have analyzed the harmonic oscillator model of aromaticity (HOMA), magnetic index, and nuclear index chemical shift (NICS) to know the

https://doi.org/10.1021/acsomega.4c01545
ACS Omega 2024, 9, 24831−24844

Table 5. Computed HOMA and NICS Aromaticity Indices for the Most Stable Complexes[a]

	5FU			A/G			T/C		
complex	HOMA	NICS(0)	NICS(1)	HOMA (6/5)	NICS(0) (6/5)	NICS(1) (6/5)*	HOMA	NICS(0)	NICS(1)
5FU	0.450	−2.666	−2.468	-	-	-	-	-	-
AT	-	-	-	0.884/0.973	−5.833/−14.367	−8.209/−10.926	0.537	−1.459	−2.384
GC	-	-	-	0.824/0.874	−3.284/−13.503	−4.173/−9.128	0.712	−0.826	−2.924
HAT	-	-	-	0.974/0.889	−6.204/−14.374	−8.663/−10.725	0.539	−1.176	−2.416
HGC^+	-	-	-	0.839/0.905	−3.459/−14.327	−4.476/−10.199	0.757	−1.313	−2.537
5FU−AT	0.522	−2.940	−2.742	0.973/0.909	−5.938/−14.163	−8.021/−11.186	0.544	−1.175	−2.367
5FU−GC	0.538	−2.914	−2.736	0.887/0.876	−3.426/−16.484	−4.472/−10.541	0.713	−0.782	−2.808
5FU−HAT	0.515	−3.166	− 2.783	0.972/0.887	−6.668/−11.158	−8.557/−21.645	0.599	−2.141	−2.921
5FU−HGC^+	0.556	−3.319	− 2.992	0.906/0.895	−4.083/−15.824	−4.964/−10.483	0.744	−1.175	−2.358

[a](6/5)* represents values on the 6- and 5-membered rings.

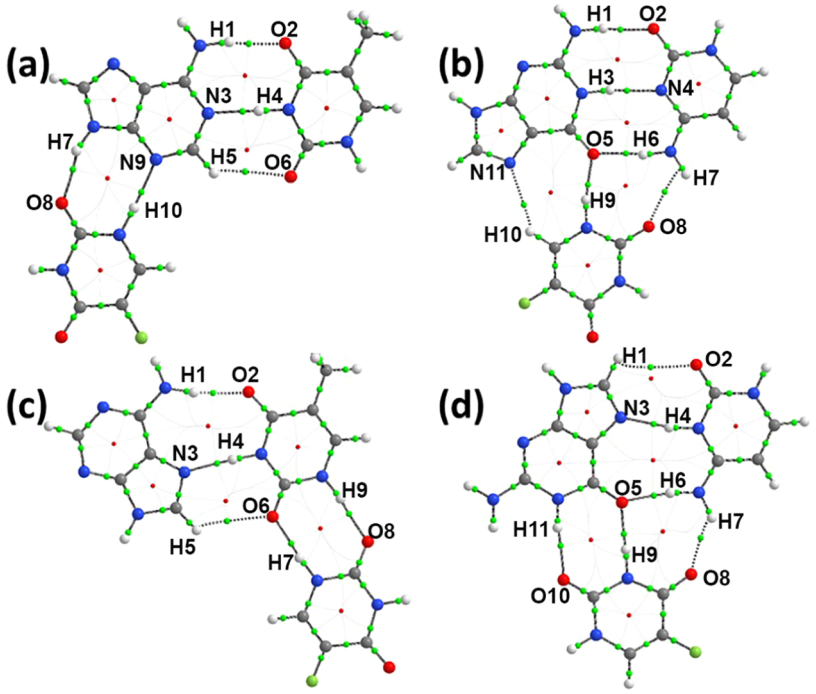

Figure 4. Molecular topography analysis for the (a) 5FU−AT, (b) 5FU−GC, (c) 5FU−HAT, and (d) 5FU−HGC^+ nucleobase pairs.

effect of 5FU binding with WC/HG base pairing.[80,81] The computed HOMA values of 5FU, AT, GC, HAT, and HGC+ are provided in Table 5. Our computed values of HOMA for AT and GC are close to the previous studies reported by Nowroozi et al.[32] The computed HOMA value on 5FU was 0.450, which upon complex formation with base pairs increases. Furthermore, the value of HOMA on 5FU is found to be proportional to the computed adsorption energy, and the highest is observed for the charged species 5FU−HGC^+ complex. In comparison between AT and HAT base pairs, the 5FU−HAT complex has a lower HOMA index on 5FU. On the contrary, the HOMA values on A and T were found to be changed depending on the site of attachment of 5FU. In the 5FU−AT complex, the HOMA values of 6- and 5-membered rings are found to increase and decrease, respectively, while thymine is practically unchanged. In the case of the 5FU−HAT complex, the HOMA value of cytosine shows an appreciable change after complexation, while adenine's 5- and 6-membered ring values are practically unchanged. This reflects that the base that is not attached to the 5FU drug in the complex offers little contribution toward π−electron delocalization.

To corroborate the above results, we have carried out NICS analysis, and its NICS(0) and NICS(1) values are provided in Table 5. The NICS values were found to be in line with the HOMA values. The extension of change in the NICS values is found to be higher for the charged 5FU−HCG^+ complex. Furthermore, the NICS(1) value for the 5FU−HCG^+ complex shows relatively less variation, likely due to the effect of charge diminishing exponentially with distance. The above results demonstrate the adsorption of 5FU on base pairing markedly increases the delocalization and is mainly localized on the base on which it gets attached and the presence of charge increases the adsorption of the 5FU drug.

3.4.3. Atom in Molecule and Noncovalent Interaction Analysis. Computing the strength of individual bonds using quantum mechanics is hostile; hence, several external methods such as bond dissociation energy, valence bond theory, molecular orbital theory, and topology of electron density are widely used.[82,83] Atoms in molecule (AIM) analysis is widely used to detect the existence of H-bonds. At the

https://doi.org/10.1021/acsomega.4c01545
ACS Omega 2024, 9, 24831−24844

Table 6. QTAIM Parameters (in a.u.) of Intermolecular Bonding between Nucleobases and between Nucleobases and the 5FU Drug Computed by the M06-2X-D3/6-311+G(d,p) Method[a]

bond	$\rho(r_{bcp})$	$\nabla^2\rho(r_{bcp})$	λ_1	λ_2	λ_3	$V(r_{bcp})$	$G(r_{bcp})$	$H(r_{bcp})$	ε	E_{HB} (in kcal mol^{-1})
					5FU−AT					
H1−O2	0.022918	0.090153	−0.030876	−0.029656	0.150686	−0.017371	0.019955	−0.002584	0.041147	5.45
N3−H4	0.045459	0.104674	−0.076009	−0.071697	0.252380	−0.040330	0.033249	0.007081	0.060147	12.65
H5−O6	0.006292	0.020151	−0.005465	−0.005401	0.031018	−0.003721	0.004380	−0.000658	0.011860	1.17
H7−O8	0.029157	0.116337	−0.042462	−0.041369	0.200169	−0.024827	0.026956	−0.002129	0.026437	7.79
N9−H10	0.040191	0.100270	−0.064227	−0.060472	0.224968	−0.033652	0.029360	0.004292	0.062096	10.56
					5FU−GC					
H1−O2	0.028662	0.111588	−0.041902	−0.039963	0.193453	−0.023910	0.025904	−0.001993	0.048511	7.50
H3−N4	0.033999	0.095314	−0.050822	−0.047702	0.193838	−0.026555	0.025192	0.001363	0.065402	8.33
O5−H6	0.030702	0.123254	−0.045998	−0.044329	0.213581	−0.027154	0.028984	−0.001830	0.037661	8.52
H7−O8	0.011191	0.049571	−0.009879	−0.006121	0.06557	−0.008071	0.010232	−0.002161	0.614084	2.53
O5−H9	0.041906	0.147140	−0.071236	−0.068629	0.287005	−0.041104	0.038945	0.002160	0.037996	12.90
N11−H10	0.008105	0.023884	−0.007082	−0.006944	0.037910	−0.004082	0.005026	−0.000944	0.019903	1.28
					5FU−HAT					
H1−O2	0.022686	0.093331	−0.030568	−0.029448	0.153347	−0.017505	0.020419	−0.002914	0.038027	5.49
N3−H4	0.044197	0.106341	−0.073551	−0.069873	0.249766	−0.039214	0.032900	0.006314	0.052630	12.30
H5−O6	0.005630	0.019825	−0.004722	−0.004413	0.028960	−0.003400	0.004178	−0.000778	0.070093	1.06
H9−O8	0.032157	0.121591	−0.049345	−0.047243	0.218178	−0.027954	0.029176	−0.001222	0.044500	8.77
O6−H7	0.038524	0.133893	−0.063093	−0.060526	0.257512	−0.035658	0.034566	0.001092	0.042418	11.18
					5FU−HGC$^+$					
H6−O5	0.037877	0.141390	−0.061351	−0.059438	0.262179	−0.036148	0.035748	0.000400	0.032175	11.34
N3−H4	0.047309	0.101331	−0.080489	−0.076940	0.258761	−0.042131	0.033732	0.008399	0.046127	13.22
O2−H1	0.005088	0.020247	−0.004128	−0.002715	0.027091	−0.003234	0.004148	−0.000914	0.520246	1.01
H7−O8	0.015268	0.063218	−0.016913	−0.016139	0.096270	−0.010563	0.013184	−0.002621	0.047934	3.31
O5−H9	0.044274	0.151506	−0.076348	−0.073725	0.301579	−0.044278	0.041077	0.003201	0.035591	13.89
H11−O10	0.027623	0.105371	−0.039698	−0.038219	0.183287	−0.022280	0.024311	−0.002031	0.038693	6.99

[a]The atomic numbering is provided in Figure 4.

intermolecular bond critical points (BCPs), the electron density ($\rho(r_{bcp})$), their Laplacians ($\nabla^2\rho(r_{bcp})$), and the energetic properties ($H(r_{bcp})$) allow us to categorize the interactions.[84] For hydrogen bonds, $\nabla^2\rho(r_{bcp})$ is positive, $V(r_{bcp})$ is negative, and $G(r_{bcp})$ and $H(r_{bcp})$ are positive values. When $\nabla^2\rho(r_{bcp})$ and $H(r_{bcp})$ are positive, a weak noncovalent hydrogen bond is elucidated.

The tomographs obtained for all of the 5FU stable complexes are depicted in Figure 4. The topological values for the intermolecular BCPs between bases and 5FU and base pairing are provided in Table 6.

The $\rho(r_{bcp})$ values on the intermolecular BCPs for the interaction between 5FU and base pairings were in the range of 0.008−0.044 au, which is close to the values proposed by Popelier and Koch for hydrogen bonding.[85] In general, $\rho(r)$ values of C═O···H−N-type interactions are higher than that of N···H/N−H···O. The amine N−H···O═C bonds have $\rho(r_{bcp})$ values close to 0.02 au and show positive and negative values for $\nabla^2\rho(r_{bcp})$ and $H(r_{bcp})$, respectively.[86] Hence, the N−H···O═C intermolecular bonds between the base pair and the 5FU drug and between the nucleobases can be categorized as medium hydrogen bonds with partial covalent character. A similar conclusion can be reached for the C−H···O═C intermolecular bonds between the base pairs even though the $\rho(r)$ values are <0.01 au. The N···H intermolecular bonds between the base pair/drug and nucleobases are weak, closed shell interactions and electrostatic interactions, as they show positive values for $\nabla^2\rho(r_{bcp})$ and $H(r_{bcp})$.

The ellipticity (ε) at any BCP measures the extent to which charge is accumulated, thereby providing a measure for the stability of the bond. A BCP with a substantially higher ellipticity value means the bond can easily undergo rupture due to charge accumulation.[87] Thus, electrostatic interactions including van der Waals interaction will have larger ellipticity than hydrogen bonds. From the table, it is evident that N···H intermolecular bonds have higher ellipticity values and electrostatic nature.[88] Furthermore, the ratio of $\left|\frac{-V(bcp)}{G(bcp)}\right|$ is >0.7 for the above bonds, which indicates the presence of strong electrostatic contribution. The computed HB energy using the empirical relation $E_{HB} = 0.5\ |V(rbcp)|$ is provided in Table 6. The E_{HB} values for all of the bonds are marginally closer to the values reported for either weak- or medium-strength bonds. A comparison between the intermolecular bond strengths between 5FU and nucleobases and among nucleobases shows that base pairs with GC have higher interaction with the 5FU drug, which is in line with our absorption energy result. For the base pairs involving AT, the E_{HB} values for the intermolecular HBs between the AT base pair and the 5FU drug are less compared to the intermolecular interaction among the A and T bases. To know the change in the strength of intermolecular interaction between base pairs after the adsorption of the 5FU drug, we compare the E_{HB} values of free base pairs (AT, GC, HAT, and HGC$^+$) with their complexes with the 5FU drug. The E_{HB} values for the free base pairs computed using Espino's method are provided in Table S3. Among the intermolecular HBs between the nucleobases, the N···H−N bond experiences an increase in bond strength values, while the other bonds show a marginal decrease. Except for the 5FU−AT complex, the summation of intermolecular

https://doi.org/10.1021/acsomega.4c01545
ACS Omega 2024, 9, 24831−24844

Table 7. Energy Decomposition Analysis for the 5FU−Nucleobase Pair, 5FU−Nucleobase, and Nucleobase Pair Complexes Computed[a,b]

system	ΔE_{Pauli}	ΔE_{elstat}	ΔE_{orbit}	ΔE_{disp}
5FU−AT	30.00	−30.82 (58.97)	−17.66 (33.79)	−3.78 (7.23)
5FU−GC	23.17	−28.33 (60.68)	−13.52 (28.96)	−4.84 (9.92)
5FU−HAT	29.37	−23.44 (56.41)	−13.99 (33.67)	−4.12 (9.92)
5FU−HGC$^+$	29.37	−37.44 (29.04)	−86.08 (66.77)	−5.40 (4.19)
5FU−A	31.26	−29.53 (58.34)	−17.13 (33.84)	−3.96 (7.82)
5FU−G	39.07	−36.84 (58.85)	−20.69 (33.05)	−5.07 (8.10)
5FU−T	23.41	23.41 (58.87)	−24.00 (33.36)	−13.60 (7.78)
AT	31.86	−28.82 (58.00)	−16.53 (33.27)	−4.34 (8.73)
GC	39.06	−42.95 (59.59)	−24.15 (33.51)	−4.97 (6.90)
HAT	30.53	−28.74 (58.87)	−15.75 (32.26)	−4.33 (8.87)
HGC$^+$	45.52	−55.28 (34.32)	−101.00 (62.71)	−4.77 (2.96)

[a]The percentage of contribution of the attractive interactions is given in parentheses. [b]All of the values reported are in kcal mol^{-1}.

HB values experiences an increase upon the complexation with the 5FU drug, which advocates the increase in the strength of these bonds.

A similar conclusion has been reached in the noncovalent interaction analysis, where H-bonding interactions are stronger and play a dominant role in stabilizing the complexes (for detailed discussion, see the Supporting Information). The RDG isosurface shown in Figure S12 also indicates that the interaction between the drug and nucleobases is stronger than the nucleobase pair bonding.

3.4.4. Energy Decomposition Analysis. Among the external methods used for computing the strength of individual bonds, energy decomposition analysis (EDA) is widely used, as it can use molecular fragments without distinct atoms in their ground state.[89] In EDA, the interaction energy (ΔE_{int}) is defined as the energy difference between the electronic energy of a whole system and the energy of its fragments in the ground-state geometry. To do so, we have used the optimized geometry of the stable 5FU−nucleobase pairs, with 5FU as one fragment and the nucleobase pair as the second fragment. We use the Ziegler-Rauk energy decomposition analysis, which is evaluated using eq 9

$$\Delta E_{int} = \Delta E_{Pauli} + \Delta E_{elst} + \Delta E_{obt} + \Delta E_{disp} \quad (9)$$

where ΔE_{Pauli} is Pauli's repulsive energy, ΔE_{elst} is the electrostatic energy, ΔE_{orb} is the orbital energy, and ΔE_{disp} is the dispersion interaction that exists between the fragments. The computed EDA results are provided in Table 7 for the 5FU interaction with the nucleobase pairing and for pristine base pairing. The results of the attractive terms are provided in terms of % contribution, which would help one to compare the various energetic terms. It is well documented that H-bonding is stabilized primarily by electrostatic interaction with a non-negligible dispersion contribution.[90,91] From Table 7, it is evident that electrostatic contribution dominates among the attractive terms except for the 5FU−HGC$^+$ complex. In the 5FU−HGC$^+$ complex, the orbital interaction accounts for nearly 66%, while the electrostatic and dispersion terms contribute to 29.04 and 4.19%, respectively. The high orbital contribution in 5FU−HGC$^+$ is because of the protonation of C, leading to cationic charge, which helps with the charge transfer and polarization effects.[59] Furthermore, due to the charged nature, the dispersion contribution is also the least in the case of the 5FU−HGC$^+$ complex.

By comparing the drug−nucleobase pair complex with nucleobase pair complexes, we notice a marginal increase in the electrostatic contributions except for the 5FU−HGC$^+$ complex. The marginal increase exemplifies the increase in H-bonding strength in the drug−nucleobase pair complexes. To compare the three systems, namely, the drug−nucleobase complex, drug−nucleobase, and the nucleobase pairs, we plotted the polar graph, which is shown in Figure S14. The orbital and dispersion contributions in all of the systems remain unchanged even after the complex formation, except for the charged Hoogsteen base pair HGC$^+$. It is evident from the polar graph that the electrostatic interactions follow the trend of drug−nucleobase < nucleobase pairs < drug−nucleobase pairs in the Watson−Crick base pairs. Thus, in WC base pairs, the highest value of electrostatic interaction observed for the drug−nucleobase pairs implies that drug interaction with nucleobase pairs leads to higher H-bond stability for the complex, while in the Hoogsteen base pairs, the H-bond stability decreases with the complexation of the 5FU drug.

4. CONCLUSIONS

The adsorption of 5-fluorouracil (5FU) on Watson−Crick (WC) base pairs (AT and GC) and Hoogsteen (HT) base pairs (HAT and HGC$^+$) was determined by adsorption energy, binding energy, and thermochemistry. The density functional theory study shows that planar geometry is more stable than the buckle angle and those with π interactions. The binding energies show that 5FU has a higher preference for WC than HT base pairs. The binding energies of 5FU on nucleobase pairs are consistently higher than those on pristine nucleobase pairs, which indicates that nucleobase pair cleavage is less likely during the adsorption of the 5FU drug. The thermodynamic parameters such as enthalpy and Gibbs free energy are all negative, which indicates that 5FU complexation with nucleobase/nucleobase pairs is exothermic and spontaneous. The electrophilicity-based charge transfer indicates that electron transfer occurs from the 5FU drug to the base pair. The MESP diagram of the stable 5FU−nucleobase pair complexes shows a directional interaction, with the positive region in a molecule interacting with the negative region of other molecules. The atoms in molecules analysis indicates that the N−H···O═C intermolecular bonds between the base pair and the 5FU drug and between the nucleobases can be categorized as medium hydrogen bonds with partial covalent character. NCI−RDG analysis depicts that H-bonding interactions are stronger and play a dominant role in stabilizing the complexes. EDA analysis shows that orbital interaction accounts for nearly 66% in the 5FU−HGC$^+$ complex because

https://doi.org/10.1021/acsomega.4c01545
ACS Omega 2024, 9, 24831−24844

of the cationic charge, which helps with charge transfer and polarization effects. The highest value of electrostatic interaction observed in 5FU−WC nucleobase pairs implies that drug interaction with nucleobase pairs leads to higher H-bond stability for the complex than in the Hoogsteen base pairs.

■ ASSOCIATED CONTENT

Supporting Information

The Supporting Information is available free of charge at https://pubs.acs.org/doi/10.1021/acsomega.4c01545.

Fully optimized geometries of low-lying isomers of drug 5FU with nucleobases and nucleobases pairs (Figures S1−S8); optimized geometries of the most stable nucleobases pairs with various functionals (Figure S9); MESP of nucleobases and base pairs (Figure S10); RDG isosurface of base pairs and 5FU−base pairs (Figure S11); NCI plots for base pairs and 5FU−base pairs (Figure S12); AIM topography of nucleobase pairs (Figure S13); polar graph on EDA analysis (Figure S14); detailed noncovalent interaction (NCI) analysis; selected vibrational frequencies for nucleobase pairs and 5FU−nucleobase pairs (Table S1); thermodynamic parameters for 5-fluorouracil with nucleobases (Table S2); and QTAIM parameters for nucleobase pairs (PDF)

■ AUTHOR INFORMATION

Corresponding Authors

Natarajan Sathiyamoorthy Venkataramanan − *Department of Chemistry, School of Engineering, Dayananda Sagar University, Bangalore, Karnataka 562112, India;* orcid.org/0000-0001-6228-0894; Email: nsvenkataramanan@gmail.com, venkataramanan-chem@dsu.edu.in

Ryoji Sahara − *Research Center for Structural Materials, National Institute for Materials Science (NIMS), Tsukuba 305-0047, Japan*; Email: SAHARA.Ryoji@nims.go.jp

Author

Ambigapathy Suvitha − *Department of Chemistry, Surana College, Bangalore 560 004, India*

Complete contact information is available at: https://pubs.acs.org/10.1021/acsomega.4c01545

Notes

The authors declare no competing financial interest.

■ ACKNOWLEDGMENTS

The author thanks the staff of the Center for Computational Materials Science, Institute for Materials Research, Tohoku University, and the supercomputer resources through the HPCI System Research Project (Project ID: hphp200040).

■ DEDICATION

†Dedicated to Professor Yoshiyuki Kawazoe on the occasion of his 75th birthday.

■ REFERENCES

(1) Carmeliet, P.; Jain, R. K. Angiogenesis in cancer and other diseases. *Nature* **2000**, *407*, 249−257.

(2) Wang, D.; Lippard, S. J. Cellular processing of platinum anticancer drugs. *Nat. Rev. Drug Discovery* **2005**, *4*, 307−320.

(3) Grothey, A.; Sargent, D.; Goldberg, R. M.; Schmoll, H.-J. Survival of patients with advanced colorectal cancer improves with the availability of fluorouracil-Leucovorin, Irinotecan, and oxaliplatin in the course of treatment. *J. Clin. Oncol.* **2004**, *22*, 1209−1214.

(4) Longley, D. B.; Harkin, D. P.; Johnston, P. G. 5-Fluorouracil: mechanisms of action and clinical strategies. *Nat. Rev. Cancer* **2003**, *3*, 330−338.

(5) Vincent, J.; Mignot, G.; Chalmin, F.; Ladoire, S.; Bruchard, M.; Chevriaux, A.; Martin, F.; Apetoh, L.; Rébé, C.; Ghiringhelli, F. 5-Fluorouracil selectively kills tumor-associated myeloid-derived suppressor cells resulting in enhanced T cell-dependent antitumor immunity. *Cancer Res.* **2010**, *70*, 3052−3061.

(6) Longley, D. B.; Johnston, P. G. Molecular mechanisms of drug resistance. *J. Pathol.* **2005**, *205*, 275−292.

(7) Wilson, P. M.; Danenberg, P. V.; Johnston, P. G.; Lenz, H.-J.; Ladner, R. D. *Nat. Rev. Clin. Oncol.* **2014**, *11*, 282−298.

(8) Vodenkova, S.; Buchler, T.; Cervena, K.; Veskrnova, V.; Vodicka, P.; Vymetalkova, V. 5-fluorouracil and other fluoropyrimidines in colorectal cancer: past, present and future. *Pharmacol. Ther.* **2020**, *206*, No. 107447.

(9) Wyatt, M. D.; Wilson, D. M., III Participation of DNA repair in the response to 5-fluorouracil. *Cell. Mol. Life Sci.* **2009**, *66*, 788−799.

(10) Watson, J. D.; Crick, F. H. C. The Structure of DNA. *Cold Spring Harbor Symp. Quant. Biol.* **1953**, *18*, 123−131.

(11) Hoogsteen, K. The crystal and molecular structure of a hydrogen-bonded complex between 1-methylthymine and 9-methyladenine. *Acta Crystallogr.* **1963**, *16*, 907−916.

(12) Vreede, J.; Ortíz, A. P.; Bolhuis, P. G.; Swenson, D. W. H. Atomistic insight into the kinetic pathways for Watson-Crick to Hoogsteen transitions in DNA. *Nucleic Acids Res.* **2019**, *47*, 11069−11076.

(13) Alvey, H. S.; Gottardo, F. L.; Nikolova, E. N.; Al-Hashimi, H. M. Widespread transient Hoogsteen base pairs in canonical duplex DNA with variable energetics. *Nat. Commun.* **2014**, *5*, No. 4786.

(14) Sánchez-González, A.; Grenut, P.; Gil, A. Influence of conventional hydrogen bonds in the intercalation of phenathroline derivatives with DNA: the important role of the sugar and phosphate backbone. *J. Comput. Chem.* **2022**, *43*, 804−821.

(15) Almaqwashi, A. A.; Paramanathan, T.; Rouzina, I.; Williams, M. C. Mechanisms of small molecule − DNA interactions probed by single−molecule force spectroscopy. *Nucleic Acids Res.* **2016**, *44*, 3971−3988.

(16) Khan, G. S.; Shah, A.; Rehman, Z.-u.; Barker, D. Chemistry of DNA minor groove binding agents. *J. Photochem. Photobiol., B* **2012**, *115*, 105−118.

(17) Snyder, R. D. Assessment of atypical DNA intercalating agents in biological and in silico systems. *Mutat. Res., Fundam. Mol. Mech. Mutagen.* **2007**, *623*, 72−82.

(18) Snyder, R. D.; Hendry, L. B. Toward a greater appreciation of noncovalent chemical/DNA interactions: Application of biological and computational approaches. *Environ. Mol. Mutagen.* **2005**, *45*, 100−105.

(19) Mallajosyula, S. S.; Datta, A.; Pati, S. K. Structure and electronic properties of the Watson-Crick base pairs: Role of hydrogen bonding. *Synth. Met.* **2005**, *155*, 398−401.

(20) Roca-Sanjuán, D.; Merchán, M.; Serrano-Andrés, L.; Rubio, M. Ab initio determination of the electron affinities of DNA and RNA nucleobases. *J. Chem. Phys.* **2008**, *129*, No. 095104.

(21) Panigrahi, S.; Pal, R.; Bhattacharyya, D. Structure and energy of non-canonical basepairs: comparison of various computational chemistry methods with crystallographic ensembles. *J. Biomol. Struct. Dyn.* **2011**, *29*, 541−556.

(22) Fan, W. J.; Zhang, R. Q.; Liu, S. Computation of large systems with an economic basis set: structures and reactivity indices of nucleic acid base pairs from density functional theory. *J. Comput. Chem.* **2007**, *28*, 967−974.

(23) Brovarets, O. O.; Yurenko, Y. P.; Hovorun, D. M. Intermolecular CH···O/N-H bonds in the biologically important pairs of natural nucleobases: a through quantum-chemical study. *J. Biomol. Struct. Dyn.* **2014**, *32*, 993−1022.
(24) Masoodi, H. R.; Bagheri, S.; Abareghi, M. The effects of tautomerization and protonation on the adenine···cytosine mismatches: a density functional theory study. *J. Biomol. Struct. Dyn.* **2016**, *34*, 1143−1155.
(25) Shi, Y.; Jiang, W.; Zhang, Z.; Wang, Z. Cooperative vibrational properties of hydrogen bonds in Watson-Crick DNA base pairs. *New J. Chem.* **2017**, *41*, 12104−12109.
(26) Geronimo, I.; Vivo, M. D. Alchemical free-energy calculations of Watson-Crick and Hoogsteen base pairing interconversion in DNA. *J. Chem. Theory Comput.* **2022**, *18*, 6966−6973.
(27) Deepa, P.; Kolandaivel, P.; Senthilkumar, K. Interactions of anticancer drugs with usual and mismatch base pairs − density functional theory studies. *Biophys. Chem.* **2008**, *136*, 50−58.
(28) Shankar, R.; Radhika, R.; Thangamani, D.; Kumar, L. S.; Kolandaivel, P. Theoretical studies on interactions of anticancer drugs (dacarbazine, procarbazine and triethylenemelamine) with normal (AT and GC) and mismatch (GG, CC, AA and TT) base pairs. *Mol. Simul.* **2015**, *41*, 633−652.
(29) Qiu, Z.; Xia, Y.; Wang, H.; Diao, K. MP2 study on the hydrogen-bonding interactions between 4-thiouracil and four RNA bases. *Struct. Chem.* **2010**, *21*, 99−105.
(30) Šponer, J.; Jurečka, P.; Hobza, P. Accurate interaction energies of hydrogen-bonded nucleic acid base pairs. *J. Am. Chem. Soc.* **2004**, *126*, 10142−10151.
(31) Hokmabady, L.; Raissi, H.; Khanmohammadi, A. Interactions of the 5-fluorouracil anticancer drug with DNA pyrimidine bases: a detailed computational approach. *Struct. Chem.* **2016**, *27*, 487−504.
(32) Nakhaei, E.; Nowroozi, A.; Ravari, F. The influence of 5-fluorouracil anticancer drug on the DNA base paris; a quantum chemical study. *J. Biomol. Struct. Dyn.* **2019**, *37*, 1−19.
(33) Ahmed, B.; Barukial, P.; Bezbaruah, B. Some halogenated anticancer agents, role of halide (-X) and their interaction mechanism with AT/GC base pairs: a computational study. *J. Indian Chem. Soc.* **2023**, *100*, No. 101027.
(34) Rezaei-Sameti, M.; Borojeni, I. Z. Interaction of 5-fluorouracil anticancer drug with nucleobases: insight from DFT, TD-DFT, and AIM calculations. *J. Biomol. Struct. Dyn.* **2023**, *41*, 5882−5893.
(35) Frisch, M. J.; Trucks, G. W.; Schlegel, H. B.; Scuseria, G. E.; Robb, M. A.; Cheeseman, J. R.; Scalmani, G.; Barone, V.; Petersson, G. A.; Nakatsuji, H.; Li, X.; Caricato, M.; Marenich, A. V.; Bloino, J.; Janesko, B. G.; Gomperts, R.; Mennucci, B.; Hratchian, H. P.; Ortiz, J. V.; Izmaylov, A. F.; Sonnenberg, J. L.; Williams-Young, D.; Ding, F.; Lipparini, F.; Egidi, F.; Goings, J.; Peng, B.; Petrone, A.; Henderson, T.; Ranasinghe, D.; Zakrzewski, V. G.; Gao, J.; Rega, N.; Zheng, G.; Liang, W.; Hada, M.; Ehara, M.; Toyota, K.; Fukuda, R.; Hasegawa, J.; Ishida, M.; Nakajima, T.; Honda, Y.; Kitao, O.; Nakai, H.; Vreven, T.; Throssell, K.; Montgomery, J. A., Jr.; Peralta, J. E.; Ogliaro, F.; Bearpark, M. J.; Heyd, J. J.; Brothers, E. N.; Kudin, K. N.; Staroverov, V. N.; Keith, T. A.; Kobayashi, R.; Normand, J.; Raghavachari, K.; Rendell, A. P.; Burant, J. C.; Iyengar, S. S.; Tomasi, J.; Cossi, M.; Millam, J. M.; Klene, M.; Adamo, C.; Cammi, R.; Ochterski, J. W.; Martin, R. L.; Morokuma, K.; Farkas, O.; Foresman, J. B.; Fox, D. J. *Gaussian 16*, Rev. C.01; Gaussian Inc., 2016.
(36) Zhang, J.; Dolg, M. Global optimization of clusters of rigid molecules using the artificial bee colony algorithm. *Phys. Chem. Chem. Phys.* **2016**, *18*, 3003−3010.
(37) Zhang, J.; Dolg, M. ABCluster: The artificial bee colony algorithm for cluster global optimization. *Phys. Chem. Chem. Phys.* **2015**, *17*, 24173−24181.
(38) Walker, M.; Harvey, A. J. A.; Sen, A.; Dessent, C. E. H. Performance of M06, M06-2X, and M06-HF density functionals for conformationally flexible anionic clusters: M06 functionals perform better than B3LYP for a model system with dispersion and ionic hydrogen-bonding interactions. *J. Phys. Chem. A* **2013**, *117*, 12590−12600.
(39) Hohenstein, E. G.; Chill, S. T.; Sherrill, C. D. Assessment of the performance of the M05-2X and M06-2X exchange-correlation functionals for noncovalent interactions in biomolecules. *J. Chem. Theory Comput.* **2008**, *4*, 1996−2000.
(40) Zhao, Y.; Truhlar, D. G. The M06 suite of density functionals for main group thermochemistry, thermochemical kinetics, noncovalent interactions, excited states, and transition elements: Two new functionals and systematic testing of four M06-class functionals and 12 other functionals. *Theor. Chem. Acc.* **2008**, *120*, 215−241.
(41) Vydrov, O. A.; Scuseria, G. E. Assessment of a long range corrected hybrid functional. *J. Chem. Phys.* **2006**, *125*, No. 234109.
(42) Adamo, C.; Barone, V. Toward reliable density functional methods without adjustable parameters: the PBE0 model. *J. Chem. Phys.* **1999**, *110*, 6158−6170.
(43) Chai, J.-D.; Head-Gordon, M. Systematic optimization of long-range corrected hybrid density functionals. *J. Chem. Phys.* **2008**, *128*, No. 081406.
(44) Venkataramanan, N. S.; Suvitha, A.; Mizuseki, H.; Kawazoe, Y. Computational study on the interactions of mustard gas with cucurbituril macrocycles. *Int. J. Quantum Chem.* **2015**, *115*, 1515−1525.
(45) Bulat, F. A.; Toro-Labbé, A.; Brinck, T.; Murray, J. S.; Politzer, P. Quantitative analysis of molecular surfaces: Areas, volumes, electrostatic potentials and average local ionization energies. *J. Mol. Model.* **2010**, *16*, 1679−1691.
(46) Murray, J. S.; Politzer, P. The electrostatic potential: An overview. *WIREs Comput. Mol. Sci.* **2011**, *1*, 153−163.
(47) Venkataramanan, N. S.; Suvitha, A.; Sahara, R.; Kawazoe, Y. Unveiling the gemcitabine drug complexation with cucurbit[n]urils (n = 6−8): a computational analysis. *Struct. Chem.* **2023**, *34*, 1869−1882.
(48) Pooventhiran, T.; Cheriet, M.; Bhattacharyya, U.; Irfan, A.; Puchta, R.; Sowirajan, S.; Thomas, R. Detailed Structural Examination, Quantum Mechanical Studies of the Aromatic Compound Solarimfetol and Formation of Inclusion Compound with Cucurbituril. *Polycyclic Aromat. Compd.* **2022**, *42*, 5443−5455.
(49) Khalilov, L. M.; Tulyabaev, A. R.; Yanybin, V. M.; Tuktarov, A. R. 1H and 13C NMR chemical shift assignments of spirocycloalkylidenehomo- and methanofullerenes by the DFT-GIAO method. *Magn. Reson. Chem.* **2011**, *49*, 378−384.
(50) Chen, Z.; Wannere, C. S.; Corminboeuf, C.; Puchta, R.; von Ragué Schleyer, P. Nucleus-Independent chemical shifts (NICS) as an aromaticity criterion. *Chem. Rev.* **2005**, *105*, 3842−3888.
(51) Fallah-Bagher-Shaidaei, H.; Wannere, C. S.; Corminboeuf, C.; Puchta, R.; Schleyer, P. V. R. *Org. Lett.* **2006**, *8*, 863−866.
(52) Keith, T. A. *AIMAll*, Version 17.01.25; TK Gristmill Software: Overland Park KS, USA, 2017.
(53) Lu, T.; Chen, F. Multiwfn: a multifunctional wavefunction analyzer. *J. Comput. Chem.* **2012**, *33*, 580−592.
(54) Zhurko, G. A.; Zhurko, D. A. Chemcraft. http://www.chemcraftprog.com/.
(55) te Velde, G.; Bickelhaupt, F. M.; Baerends, E. J.; Guerra, C. F.; van Gisbergen, S. J. A.; Snijders, J. G.; Ziegler, T. Chemistry with ADF. *J. Comput. Chem.* **2001**, *22*, 931−967.
(56) Venkataramanan, N. S.; Suvitha, A.; Kawazoe, Y. Intermolecular interaction in nucleobase and dimethyl sulfoxide/water molecules: a dft, nbo, aim and nci analysis. *J. Mol. Graphics Modell.* **2017**, *78*, 48−60.
(57) Wielińska, J.; Nowacki, A.; Liberek, B. 5-Fluorouracil − Complete insights into the neutral and ionised forms. *Molecules* **2019**, *24*, No. 3683.
(58) Brovarets, O. O.; Hovorun, D. M. Can tautomerization of the A.T Watson-Crick base pair via double proton transfer provoke point mutations during DNA replication? A comprehensive QM and QTAIM analysis. *J. Biomol. Struct. Dyn.* **2014**, *32*, 127−154.
(59) Kumawat, R. L.; Sherrill, C. D. High-order quantum mechanical analysis of hydrogen bonding in Hachimoji and natural DNA base pairs. *J. Chem. Inf. Model.* **2023**, *63*, 3150−3157.

https://doi.org/10.1021/acsomega.4c01545
ACS Omega 2024, 9, 24831−24844

(60) Grabowski, S. J. Ab initio calculations on conventional and unconventional hydrogen bonds − study of the hydrogen bond strength. *J. Phys. Chem. A* **2001**, *105*, 10739−10746.
(61) Beiranvand, N.; Freindorf, M.; Kraka, E. Hydrogen bonding in natural and unnatural base pairs- a local vibrational mode study. *Molecules* **2021**, *26*, No. 2268.
(62) Venkataramanan, N. S.; Suvitha, A.; Nejo, H.; Mizuseki, H.; Kawazoe, Y. Electronic structure and spectra of symmetric meso-substituted porphyrin: dft and tddft-PCM investigations. *Int. J. Quantum Chem.* **2011**, *111*, 2340−2351.
(63) Silva, A. L. P.; de Jesus Gomes Varela Júnior, J. Density functional theory study of Cu-Modified B12N12 nanocage as a chemical sensor for carbon monoxide gas. *Inorg. Chem.* **2023**, *62*, 1926−1934.
(64) Yar, M.; Shah, A. B.; Hashmi, M. A.; Ayub, K. Selective detection and removal of picric acid by C2N surface from a mixture of nitro-explosives. *New J. Chem.* **2020**, *44*, 18646−18655.
(65) de Sousa Sousa, N.; Silva, A. L. P.; Silva, A. C. A.; de Jesus Gomes Varela Júnior, J. Cu-modified B12N¬12 nanocage as a chemical sensor for nitrogen monoxide gas: a density functional theory study. *J. Nanopart. Res.* **2023**, *25*, No. 248.
(66) Nair, R. G. S.; Nair, A. K. N.; Sun, S. Adsorption of gases on fullerene-like X12Y12 (X = Be, Mg, Ca, B, Al, Ga, C; Y = C, Si, N, P, O) nanocages. *Energy Fuels* **2023**, *37*, 14053−14063.
(67) Phung, V. B. T.; Tran, T. N.; Tran, Q. H.; Luong, T. T.; Dinh, V. A. Graphene as sensor for lung cancer: insights into adsorption of VOCs using vdw DFT. *ACS Omega* **2024**, *9*, 2302−2313.
(68) Roos, G.; Murray, J. S. Intramolecular repulsion visible through the electrostatic potential in disulfides; analysis via varying iso-density envelopes. *J. Phys. Chem. A* **2023**, *127*, 8354−8364.
(69) Gassoumi, B.; Ahamed, M. A. M.; Nasr, S.; Karayel, A.; Özkinali, S.; Castro, M. E.; Melendez, F. J.; Mahdouani, M.; Nouar, L.; Madi, F.; Ghalla, H.; Bourguiga, R.; et al. Revealing the effect of Co/Cu (d7/d9) cationic doping on an electronic acceptor ZnO nanocage surface for the adsorption of citric acid, vinyl alcohol, and sulfamethoxazole ligands: DFT-D3, QTAIM, IGM-NCI and MD analysis. *Mater. Chem. Phys.* **2023**, *309*, No. 128364.
(70) Gassoumi, B.; Dlala, N. A.; Echabaane, M.; Karayel, A.; Özkinali, S.; Castro, M. E.; Melendez, F. Z.; Ghalla, H.; Nouar, L.; Madi, F.; Ben, C. R. Stability, spectroscopic, electrochemistry and QTAIM analysis of Cu-Znn-1On clusters, for glucose sensing application: A study on theoretical and experimental insights. *Heliyon* **2022**, *8*, No. e12387.
(71) Dobrowolski, J. C.; Ostrowski, S. HOMA index establishes similarity to a reference molecule. *J. Chem. Inf. Model.* **2023**, *63*, 7744−7754.
(72) Srivastava, A. K. Boronyl-based polycyclic superhalogens. *J. Phys. Chem. A* **2023**, *127*, 10406−10411.
(73) Venkataramanan, N. S.; Suvitha, A.; Rahim, S. A.; Sahara, R. Intermolecular hydrogen bond interactions in water clusters of zwitterionic glycine: dft, mesp, aim, rdg and molecular dynamics. *J. Mol. Liq.* **2024**, *396*, No. 123932.
(74) Yar, M.; Ahsan, F.; Gulzar, A.; Ayub, K. Adsorption and sensor application of C2N surface for G-series and mustard series chemical warfare agents. *Microporous Mesoporous Mater.* **2021**, *317*, No. 110984.
(75) Echeverria, J. Cooperative effects between hydrogen bonds and C═O···S interactions in the crystal structures of sulfoxides. *Cryst. Growth Des.* **2021**, *4*, 2481−2487.
(76) Donald, K. J.; Pham, N.; Ravichandran, P. Sigma hole potentials as tools: quantifying and partitioning substituent effects. *J. Phys. Chem. A* **2023**, *127*, 10147−10158.
(77) Al-Wahaibi, L. H.; Karthikeyan, S.; Blacque, O.; El-Masry, A. A.; Hassan, H. H.; Percino, M. J.; El-Emam, A. A.; Thamotharan, S. Structural and energies properties of weak noncovalent interactions in two closely related 3,6-disubstituted-[1,2,4]triazolo[3,4-b][1,3,4] thiadiazole derivatives: In vitro cyclooxygenase activity, crystallography and computational investigations. *ACS Omega* **2022**, *7*, 34506−34520.
(78) Anjali, B. A.; Suresh, C. H. Interpreting oxidative addition of Ph-X (X═CH3, F, Cl, and Br) to monoligated Pd(0) catalysts using molecular electrostatic potential. *ACS Omega* **2017**, *2*, 4196−4206.
(79) Majhi, B.; Lohar, V. A.; Meena, P.; Chopra, D. Quantitative investigations of intermolecular Te···A (A = π/Te/H) interactions in organotellurium compounds from the Cambridge structural database. *Cryst. Growth Des.* **2023**, *23*, 7922−7938.
(80) Antić, M.; Furtula, B.; Radenković, S. Aromaticity of nonplanar fully benenoid hydrocarbons. *J. Phys. Chem. A* **2017**, *121*, 3616−3626.
(81) Baranac-Stojanović, M.; Aleksić, J.; Stojanović, M. Theoretical investigation of tautomerism of 2- and 4-pyridones: origin, substituent and solvent effects. *Org. Biomol. Chem.* **2023**, *22*, 144−158.
(82) Das, P.; Rao, G. B. D.; Bhandary, S.; Mandal, K.; Seth, S. K.; Chopra, D. Quantitative investigation into the role of intermolecular interactions in crystalline fluorinated triazoles. *Cryst. Growth Des.* **2024**, *24*, 703−721.
(83) Popelier, P. L. A. Non-covalent interactions from a quantum chemical topological perspective. *J. Mol. Model.* **2022**, *28*, No. 276.
(84) Anconi, C. P. A. Relative position and relative rotation in supramolecular systems through the analysis of the principal axes of inertia: ferrocene/cucurbit[7]uril and ferrocenyl azide/β-cyclodextrin case studies. *ACS Omega* **2020**, *5*, 5013−5025.
(85) Koch, U.; Popelier, P. L. A. Characterization of C-H-O hydrogen bonds on the basis of the charge density. *J. Phys. Chem. A* **1995**, *99*, 9747−9754.
(86) Mahadevi, A. S.; Sastry, G. N. Cooperativity in noncovalent interactions. *Chem. Rev.* **2016**, *116*, 2775−2825.
(87) Gajalakshmi, D.; Tamilmani, V.; Ebenezer, C.; Solomon, R. V. Conjugation-modulated optoelectronic and anti-corrosion properties of pyrrole oligomer: Insights from DFT/TD-DFT analysis. *J. Mol. Struct.* **2024**, *1295*, No. 136722.
(88) Afahanam, L. E.; Louis, H.; Benjamin, I.; Gber, T. E.; Ikot, I. J.; Manicum, A.-L. E. Heteroatom (B, N, P and S) − doped cyclodextrin as a hydroxyurea (HU) drug nanocarrier: a computational approach. *ACS Omega* **2023**, *8*, 9861−9872.
(89) Hobza, P.; Šponer, J. Structure, energetics, and dynamics of the nucleic acid base pairs: nonemperical ab initio calculations. *Chem. Rev.* **1999**, *99*, 3247−3276.
(90) Jurečka, P.; Šponer, J.; Černy, J.; Hobza, P. Benchmark database of accurate (MP2 and CCSD(T) complete basis set limit) interaction energies of small model complexes, DNA base pairs, and amino acid pairs. *Phys. Chem. Chem. Phys.* **2006**, *8*, 1985−1993.
(91) Karabiyik, H.; Sevincek, R.; Karabiyik, H. π-cooperativity effect on the base staking interactions in DNA: is there a novel stabilization factor coupled with base pairing H-bonds? *Phys. Chem. Chem. Phys.* **2014**, *16*, 15527−15538.

https://doi.org/10.1021/acsomega.4c01545
ACS Omega 2024, 9, 24831−24844